Available online at www.sciencedirect.com

ScienceDirect

Energy Procedia 148 (2018) 631–638

Energy Procedia

www.elsevier.com/locate/procedia

73rd Conference of the Italian Thermal Machines Engineering Association (ATI 2018), 12–14 September 2018, Pisa, Italy

Impact of the laminar flame speed correlation on the results of a quasi-dimensional combustion model for Spark-Ignition engine

Teodosio L. [a]*, Bozza F.[a], Tufano D.[a], Giannattasio P.[b], Distaso E.[c], Amirante R.[c]

[a]*Industrial Engineering Department, University of Naples "Federico II", Via Claudio 21, 80125 Naples, Italy*
[b]*Polytechnic Department of Engineering and Architecture, University of Udine, Via delle Scienze 206, I-33100 Udine, Italy*
[c]*Department of* Mechanics*, Mathematics and Management (DMMM), Polytechnic of Bari, Via Re David 200, 70126 Bari, Italy,*

Abstract

In the present study, the impact of the laminar flame speed correlation on the prediction of the combustion process and performance of a gasoline engine is investigated using a 1D numerical approach. The model predictions are compared with experimental data available for full- and part-load operations of a small-size naturally aspirated Spark-Ignition (SI) engine, equipped with an external EGR circuit.
A 1D model of the whole engine is developed in the GT-Power™ environment and is integrated with refined sub-models of the in-cylinder processes. In particular, the combustion is modelled using the fractal approach, where the burning rate is directly related to the laminar flame speed.
In this work, three laminar flame speed correlations are assessed, including both experimentally- and numerically-derived formulations, the latter resulting from the fitting of laminar flame speeds computed by a chemical kinetic solver.
Each correlation is implemented within the combustion sub-model, which is properly tuned to reproduce the experimental performance of the engine at full load. Then, the reliability of the considered flame speed formulations is proved at part-loads, even under external EGR operations.

Keywords: SI engine, 1D model, quasi-dimensional combustion modelling, laminar flame speed, EGR

* Corresponding author. Tel.: +39081-7683285; fax: +39 081 2394165.
E-mail address: luigi.teodosio@unina.it

10.1016/j.egypro.2018.08.151

Nomenclature

Acronyms

0D/1D/3D	zero/one/three dimensional
BMEP	Brake Mean Effective Pressure
BSFC	Brake Specific Fuel Consumption
CAD	Crank Angle Degree/Computer Aided Design
CFD	Computational Fluid Dynamics
EGR	Exhaust Gas Recirculation
ICE	Internal Combustion Engine
MFB_{0-10}	0-10% combustion duration
MFB_{10-50}	10-50% combustion duration
MFB_{50-90}	50-90% combustion duration
MSE	Mean Squared Error
PFI	Port Fuel Injection
SI	Spark-Ignition engine

Symbols

A_L	Flame front laminar area
A_T	Flame front turbulent area
c_{d3}	Fractal dimension multiplier
D_3	Flame front fractal dimension
$L_{Gibs,}$	Gibson length scale
L_{max}	Flame wrinkling maximum scale
L_{min}	Flame wrinkling minimum scale
m_b	Burned mass
S_L	Laminar flame speed
t	Time
X_{EGR}	Molar fraction of EGR
X_{EGRm}	Mass fraction of EGR

Greeks

ρ_u	Density of the unburned gas

1. Introduction

Nowadays, stringent regulations force car manufacturers to explore innovative and sometimes very complex technical solutions to limit pollutant and CO_2 emissions from Internal Combustion Engines (ICEs) [1]. On the other hand, “fun-to-drive” cars and improved engine performance, in terms of both fuel consumption and power/torque, are also required by the customers.

The technical solutions can be tested by experimental campaigns and/or-numerical simulations. The latter play an increasingly important role in the development stage of a new engine architecture, since they allow considerable cost and time savings. In particular, the 0D/1D simulation tools, when compared to 3D CFD models, demonstrate to be effective in reproducing the engine behaviour under different operating conditions with a much lower computational cost [2].

However, the reliability of a 0D/1D model strongly depends on the quality of the adopted sub-models, with a special reference to the turbulent combustion one. In this regard, quasi-dimensional combustion models for the prediction of the burning rate are widely employed. Although these models are based on different approaches, all of

them strongly depend on the adopted correlation for the laminar flame speed (S_L). Various laminar flame speed formulations for gasoline have been suggested in the past by different authors [3]-[9]. As an example, Metghalchi et al.[3], and Rhodes et al. [4] proposed widely used experimental correlations of the flame speed, based on a power law formula. Their main limitations lie in neglecting the cross influence of pressure and temperature and in predicting a monotonic dependency of S_L on the equivalence ratio (Φ). Some authors [5], [6] proposed improved versions of Metghalchi and Rhodes models, but also their correlations have the main drawback of being experimental-based formulations: direct measurements of laminar flame speeds are commonly performed in a limited range of equivalence ratios and at low pressures, because of technical limitations, as discussed in [7], [8]. As a consequence, these correlations may lead to inaccurate predictions when applied outside the measurement range, such as in the case of the high pressures and temperatures typical of SI engine operations.

To overcome the aforementioned issues, alternative laminar flame speed models, based on reaction kinetic calculations, were presented by Bougrine et al. [7] and by Hann et al. [9]. Indeed, the possibility of exploring a wider range of boundary conditions through kinetic calculations broadens the validation range of the correlation, but the accuracy of these models strongly depends on the adopted kinetic scheme.

In this study, an "in-house developed" chemical-based laminar flame speed correlation for gasoline is presented and compared with both a commonly adopted experimentally-derived formulation [3] and an experimental correlation recently proposed by the authors in a previous work [10]. The latter is, here, extended to take properly into account the effect of the in-cylinder residual gas content. A 1D engine model is developed in the GT-Power™ framework and integrated with phenomenological sub-models of turbulence, combustion and heat transfer processes. Each flame speed correlation is implemented into the combustion sub-model.

The considered engine is a small-size naturally aspirated SI engine, equipped with an external cooled EGR circuit, for which experimental data are available at full and part loads, including also EGR operations.

In a first stage, all the considered flame speed correlations are assessed over a wide range of operating conditions, such as unburned mixture temperature and pressure and EGR fraction.

In a second step, the engine model is tuned at full load for all the proposed correlations. Then, keeping the selected tuning constants unchanged, the part load conditions are investigated in order to verify the ability of the considered correlations to reproduce the combustion evolution and the engine performance, also under EGR operations.

A comparison among the simulation results at part loads, in terms of both combustion characteristic durations and performance parameters, is carried out to evaluate the quality of the in-house developed laminar flame speed correlation, on the basis of the mean squared error computed over the full range of engine operating points.

2. Model description

A detailed model of the considered engine has been developed in the GT-Power™ environment. The model is based on a 1D description of the unsteady flow inside the intake and exhaust pipes and a 0D representation of the in-cylinder processes. Phenomenological "in-house developed" sub-models of turbulence, combustion and heat transfer are implemented into the 1D code in the form of user routines.

The combustion process is modelled adopting a "two-zone" (burned and unburned gases) bi-fractal approach [11]. This sub-model takes into account both the geometry of the combustion system and the most important operating variables of the engine, including the intake valve strategy [12].

The burning rate expression in the employed bi-fractal approach takes the form:

$$\frac{dm_b}{dt} = \rho_u A_T S_L = \rho_u A_L S_L \left(\frac{A_T}{A_L}\right) = \rho_u A_L S_L \left(\frac{L_{\max}}{L_{Gibs}}\right)^{D_3-2} \left(\frac{L_{Gibs}}{L_{\min}}\right)^{(D_3-2)*c_{d3}} \quad (1)$$

where ρ_u is the unburned gas density, A_L and A_T are the area of the laminar and turbulent flame fronts and S_L is the laminar flame speed. L_{Gibs}, L_{max} and L_{min} are the characteristic length scales of the flame wrinkling, D_3 is the fractal dimension, and c_{d3} represents a tuning constant, as described better in [11]. The above parameters are estimated by a suitable turbulence sub-model discussed in [13]. This sub-model exhibits a good sensitivity to the engine operating

conditions (speed and load) and geometry (intake port orientation, bore-to-stroke ratio, compression ratio, valve arrangements), and to the intake valve strategy [12], [13].

A modified Hohenberg correlation is adopted for the heat transfer modelling, while the piston, cylinder liner and head temperatures are calculated using the simplified finite element tool available in GT-Power™.

Regarding the laminar flame speed, S_L, three different correlations for gasoline have been considered with the purpose of assessing their effectiveness in predicting the combustion process and engine performance in a wide range of operating conditions. Two of them are experimentally derived: the first one, labelled as "Cor A", is based on the well-known Metghalchi et al. approach [3], while the second one, labelled as "Cor B", is a formulation presented in a previous work by some of the present authors [10]. The third correlation, named "Cor C", is obtained from chemical kinetics simulations, as presented in [14]. All these correlations express the laminar flame speed using the power law formula:

$$S_L = S_{L0}\left(\frac{T_u}{T_0}\right)^{\alpha}\left(\frac{p}{p_0}\right)^{\beta} EGR_{factor} \tag{2}$$

where S_{L0} is the flame speed measured at reference temperature and pressure T_0 and p_0 for a given equivalence ratio, and α and β are mixture strength-dependent terms. The dependency of the three laminar flame speed correlations on pressure, temperature, ϕ and EGR mass fraction (X_{EGRm}) are depicted in Fig 1a-d.

The first correlation (Cor A) is based on the commonly used Metghalchi formulation [3], properly modified to reproduce the results shown in [5]:

$$S_{L0} = B_m + B_\phi(\phi - \phi_m)^2 \tag{3}$$

$$\alpha = \alpha_0 + \alpha_1\phi^{\alpha_2}; \beta = \beta_0 + \beta_1\phi^{\beta_2}; EGR_{factor1} = (1 - e_1 X_{EGR}^{e_2}) \tag{4}$$

where the values of the constants are listed in Table 1, and X_{EGR} represents the molar fraction of the residual exhaust gas.

In the second correlation (Cor B), term S_{L0} is modelled according to the Gülder formulation [8] (eq. 5), while exponents α and β are considered to be second-order polynomial functions of ϕ, as proposed by Liao et al. [6]:

$$S_{L0} = W\phi^{\eta} e^{-\xi(\phi-\sigma)^2} \tag{5}$$

$$\alpha = \alpha_0 + \alpha_1\phi + \alpha_2\phi^2; \beta = \beta_0 + \beta_1\phi + \beta_2\phi^2; EGR_{factor2} = e^{(e_1 X_{EGR})} \tag{6}$$

The values of the parameters, whose estimation process is reported in [10], are listed in Table 1. In this work, the impact of the residual gas, $EGR_{factor2}$, has been modelled by the authors so as to avoid the negative value of flame speed given by $EGR_{factor1}$ higher than X_{EGR}= 0.3912, as shown in [5],[9].

The last correlation (Cor C) [14] results from the fitting of 1D laminar flame speeds computed by a chemical kinetic solver (CHEMKIN) and based on the Liu et al. reaction mechanism [15] for a Toluene Reference Fuel (TRF). Where *RON* and *MON* are the fuel Research and Motor Octane Numbers, respectively, *S=RON-MON* is the fuel sensitivity, X_{EGRm} is the mass fraction of the residual exhaust gas, and all constants are reported in Table 1.

$$S_{L0} = A + B\phi + C\phi^2 + D\phi^3 + E\phi^4 \tag{7}$$

$$A = a_1 + a_2 S; B = b_1 + b_2 S; C = c_1 + c_2 S; D = d_1 + d_2 S; E = e_1 + e_2 S; \tag{8}$$

$$\alpha = \alpha_1 + \alpha_2\phi; \beta = \beta_1 + \beta_2\phi; \gamma = \gamma_1 + \gamma_2\phi; EGR_{factor3} = (1 - \kappa X_{EGRm})^{\gamma} \tag{9}$$

Table 1.Coefficients of the considered laminar flame speed correlations

Cor A [3] Experimentally-derived T_0=298 K, P_0=1.01325 bar T_{range}= [350-550 K]; P_{range}= [0.4-12 atm]; ϕ_{range}= [0.7-1.6]				Cor B [10] Experimentally-derived T_0=298 K, P_0=1.01325 bar T_{range}= [298-500 K]; P_{range}= [1-25 atm]; ϕ_{range}= [0.6-2.0]				Cor C [14] Numerically-derived T_0=423 K, P_0=1.00000 bar T_{range}= [323-473 K]; P_{range}= [1-10 bar]; ϕ_{range}= [0.7-1.6]					
B_m	0.35	β_2	2.77	W	36.82	a_0	5.93	a_1	101.7068	d_1	-1360.444	β_1	-0.3952267
B_ϕ	-0.549	β_1	0.14	η	0.22	b_2	-0.9250	a_2	-16.80694	d_2	84.03323	β_2	0.1766350
ϕ_m	1.1	β_0	-0.357	ξ	4.86	b_1	2.0120	b_1	-777.2416	e_1	340.6086	γ_1	1.311202
α_2	3.51	e_1	2.06	σ	1.11	b_0	-1.3650	b_2	76.07949	e_2	-19.61888	γ_2	0.6858792
α_1	-0.27	e_2	0.77	a_2	3.28	e_1	-3.69	c_1	1763.747	α_1	1.388656	κ	1.538489
α_0	2.4			a_1	-7.52			c_2	-125.1039	α_2	0.3742516		

Looking at Fig 1, some preliminary considerations can be drawn. “Cor B” and “Cor C” show a similar dependence of S_L on temperature and pressure (Fig 1a, b), while “Cor A” and “Cor C” exhibit a similar trend at varying ϕ. However, “Cor A” provides systematically a higher laminar flame speed. The EGR factors (Fig 1d) are comparable each other but “Cor A” shows a more pronounced decay with increasing EGR mass fraction.

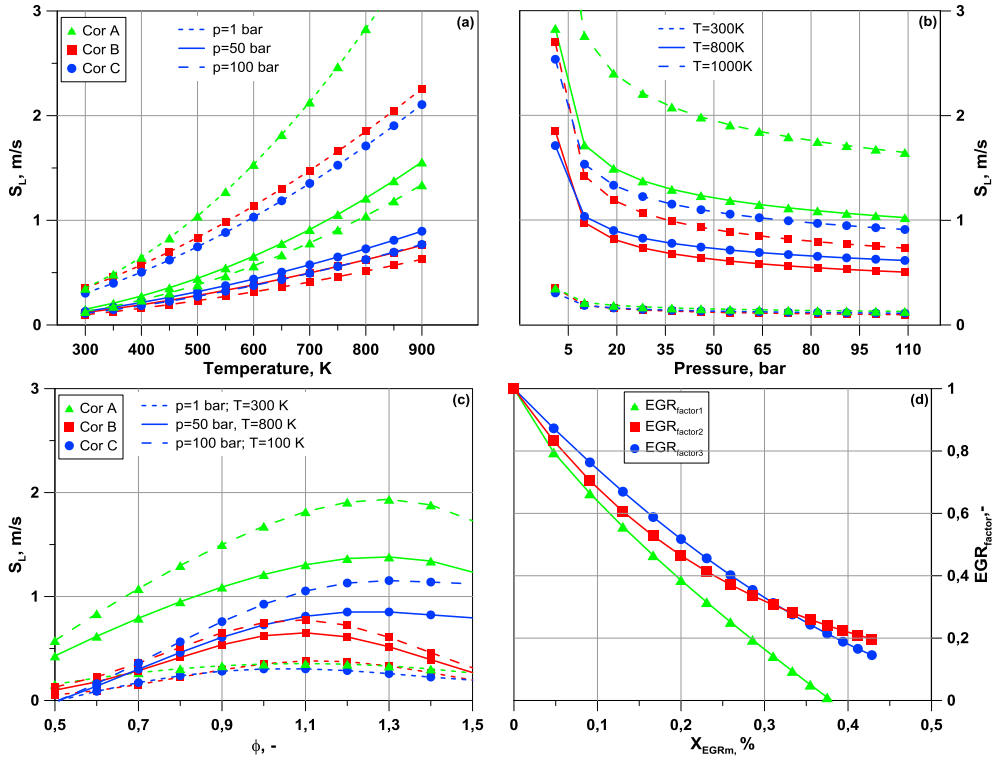

Fig 1. Dependency of the three laminar flame speed correlations on temperature (a) and pressure (b) at ϕ=1, on equivalence ratio (c), and on EGR mass fraction-(d).

3. Results Discussion: full and part load engine operations

In the 1D simulations, air-to-fuel ratio and combustion phasing (MFB_{50}) are imposed according to the experimental results, while the engine load (BMEP) is reproduced by controlling the opening of the throttle valve. The spark advance is automatically modified to match the experimental MFB_{50}. The EGR valve is controlled to reproduce the

measured external EGR flow rate. The tuning constants of the turbulence sub-model are prelimiary identified by a well-assessed procedure, based on a 1D/3D hierarchical approach, widely described in [13].

In a first stage, the combustion sub-model is tuned at full load for each flame speed correlation to reproduce the combustion process and the in-cylinder pressure cycles. In the combustion model there are three tuning constants that affect independently the different combustion stages. The first one, named c_{trans}, mainly influences the early combustion stage ($MFB_{0\text{-}10}$); the second one, named c_{wrk}, exerts localized effects on the core of combustion ($MFB_{10\text{-}50}$); the third one, x_{wc}, only affects the combustion tail ($MFB_{50\text{-}90}$). The set of the tuning constants for each laminar flame speed correlation is reported in Table 2. The constant setting of "Cor A" is quite different from the other correlations, in particular for the term c_{wrk}. This is due to the estimation of a higher laminar flame speed, as shown in Fig 1, which requires a lower value of c_{wrk} to achieve the correct combustion rate.

The tuning constants of the combustion model, identified for each flame speed correlation, are kept unchanged in the simulation of part load operating conditions, in order to prove the physical consistency of the present approach.

Table 2. Tuning constants of the combustion model for Cor A, B and C

	c_{trans}	c_{wrk}	x_{wc}		c_{trans}	c_{wrk}	x_{wc}		c_{trans}	c_{wrk}	x_{wc}
Cor A	1.34	0.48	0.5	Cor B	1.13	1.2	0.6	Cor C	1.16	0.85	0.58

The accuracy of the tuned combustion sub-model has been verified with reference to the overall performance parameters of the engine, taking into account all the flame speed correlations. For sake of brevity, the model validation is only discussed in terms of BMEP and BSFC at various engine speeds, as reported in Fig 2a-b. For confidentiality reasons, in these figures the y-axis scale is hidden-and the x-axis reports the engine speed ratio (n/n_{max}). Fig 2a-b show that the laminar flame speed correlations do not seem to affect the engine performance, as they provide equally accurate results, with a maximum absolute percentage error less than 5%. This is mainly due to the selection of a proper set of tuning constants for each correlation. The Borghi diagram, Fig 2c, highlights a different "Engine Regime" for "Cor A" when compared to "Cor B" and "Cor C", due to the estimation of higher flame speeds. However, the typical region of SI engine operation on the diagram (gray area) is covered in all cases. Other significant outcomes at full load are shown in Fig 3, which reports the main characteristic combustion durations, namely $MFB_{0\text{-}10}$, $MFB_{10\text{-}50}$ and $MFB_{50\text{-}90}$, as a function of the engine speed. The trend of $MFB_{0\text{-}10}$ is well captured by all the flame speed models, while "Cor B" and "Cor C" lead to a better agreement with the experimental speed-related trends for $MFB_{10\text{-}50}$, and $MFB_{50\text{-}90}$. In addition, the accuracy of each laminar speed formulation is evaluated computing the Mean Squared Error (MSE), σ, with respect to the experimental data. Table 3 shows the three correlations provide comparable MSEs.

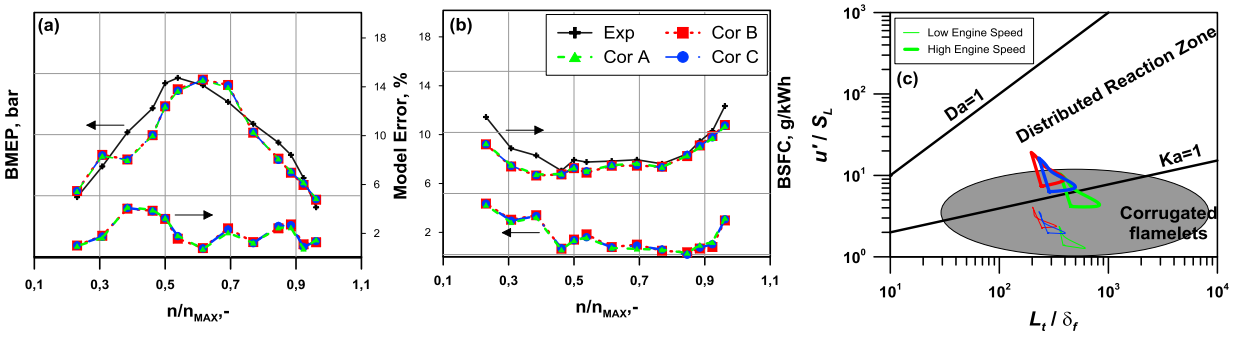

Fig 2. Numerical/experimental comparison of BMEP (a) and BSFC (b), and Borghi Diagram (c) for Cor A, B and C at full load

Table 3. MSE of the characteristic combustion durations for each flame speed correlation at full and part loads

	Full load			Part load		
	$MFB_{0\text{-}10}$	$MFB_{10\text{-}50}$	$MFB_{50\text{-}90}$	$MFB_{0\text{-}10}$	$MFB_{10\text{-}50}$	$MFB_{50\text{-}90}$
Cor A	0.56	0.53	1.42	5.04	2.03	6.77
Cor B	0.76	0.51	1.15	6.48	1.57	7.32
Cor C	0.71	0.50	1.39	6.08	1.61	7.21

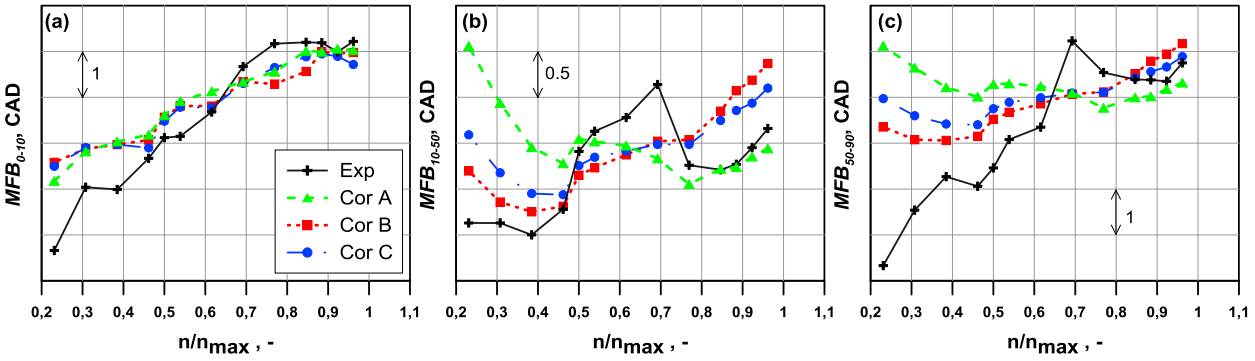

Fig 3. Characteristic combustion durations $MFB_{0\text{-}10}$ (a) $MFB_{10\text{-}50}$ (b) and $MFB_{50\text{-}90}$ (c) at full load: experimental findings vs Cor A, B and C

After tuning the combustion model at full load for each flame speed formulation, 16 part load points at various engine speeds and EGR percent ratios are investigated, as listed in Table 4.

Global model accuracy at part loads is verified in terms of fuel consumption in Fig 4a, which shows a good agreement between numerical and experimental BSFC data (model errors below 5%). "Cor A" leads to higher errors in the BSFC prediction for part load cases, Fig 4b, with an internal EGR (i-EGR) higher than the 20%. The unreliability of the EGR factor in the Metghalchi correlation for high EGR operating points is further confirmed by Fig 5a-c, where the numerical/experimental comparison of combustion durations is reported. Although the considered flame speed correlations carry out similar results at part loads, as shown in Table 3. "Cor A" provides a slightly higher MSE for $MFB_{10\text{-}50}$, which implies a worse prediction of fuel consumption. Finally, Fig 4c reports the considered part-load points at MFB_{50} angle on the Borghi Diagram. Similar considerations of the Full load case can be applied.

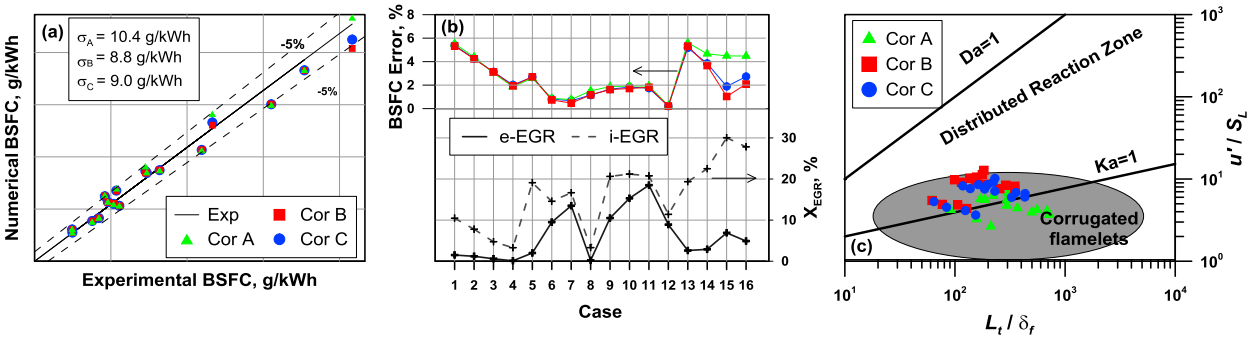

Fig 4. Numerical/experimental comparison of BSFC (a), 1D computed EGR fraction and percent BSFC error (b), and Borghi Diagram (c) for Cor A, B and C at part loads

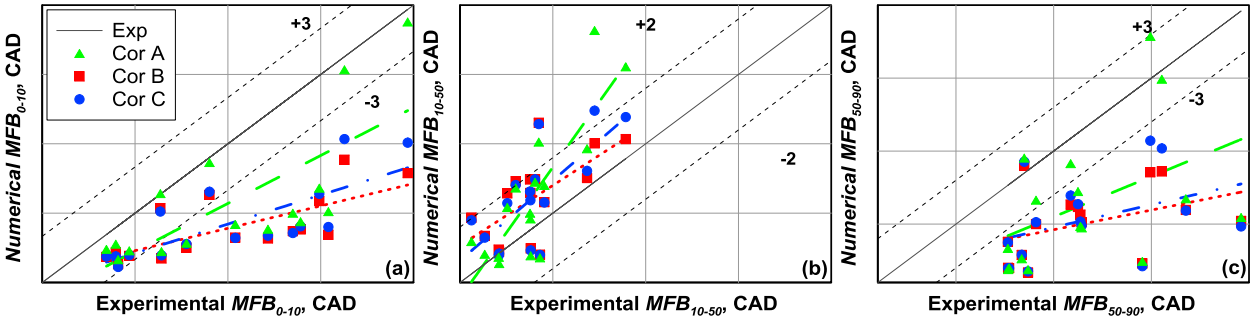

Fig 5. Characteristic combustion durations at part loads: numerical results for Cor A, B and C vs experimental findings

Table 4. Engine operating points at part load for various speeds and EGR rates

Case	1	2	3	4	5	6	7	8	9	10	11	12	13	14	15	16
n/n_{max}	0.81	0.81	0.81	0.81	0.73	0.73	0.73	0.73	0.50	0.50	0.50	0.50	0.27	0.27	0.23	0.23
$BMEP/BMEP_{max}$	0.21	0.29	0.59	0.86	0.17	0.33	0.50	0.89	0.29	0.42	0.67	0.84	0.33	0.38	0.17	0.25
EGR,%	1.47	1.20	0.65	0.14	2.02	9.54	13.47	0.17	10.52	15.34	18.54	8.87	2.59	2.86	6.93	4.90

4. Conclusions

In this work, "in-house developed" flame speed models, including both experimentally- and numerically-derived formulations, have been compared to the well-known Metghalchi correlation to assess their relative impact on the prediction of the combustion process in a SI engine.

A 1D model of a naturally aspirated gasoline engine was implemented in the GT-Power™ code and integrated with advanced sub-models of in-cylinder turbulence, combustion and heat transfer. Each flame speed correlation was implemented in the fractal combustion sub-model, which was properly tuned to reproduce the experimental performance of the engine at full load. The considered flame speed formulations provided results of comparable accuracy for the combustion evolution and engine performance at full load, whereas a slightly different engine regime was detected on the Borghi diagram for the proposed correlations compared to the Metghalchi model. The analysis of part-load operating conditions, for various speeds and EGR rates, showed a substantial equivalence of the flame speed formulations in reproducing the BSFC and the characteristic combustion durations. However, the correlations developed by the authors exhibited a better EGR-related laminar flame speed slow-down, when compared to the Metghalchi approach, resulting in more accurate predictions of combustion duration and fuel consumption at high-EGR part-load operating points.

References

[1] European Environment Agency, "Annual European Union greenhouse gas inventory 1990–2012 and inventory Report 2014, Report No.: 9/2014", 2014.
[2] da Silva Trindade, W. R., & dos Santos, R. G. (2016). Combustion Modeling Applied to Engines Using a 1D Simulation Code (No. 2016-36-0347). SAE Technical Paper.
[3] Metghalchi, M., & Keck, J. C. (1982). Burning velocities of mixtures of air with methanol, isooctane, and indolene at high pressure and temperature. Combustion and flame, 48, 191-210.
[4] Rhodes, D. B., & Keck, J. C. (1985). Laminar burning speed measurements of indolene-air-diluent mixtures at high pressures and temperatures (No. 850047). SAE Technical Paper.
[5] Hara, T., & Tanoue, K. (2006). Laminar flame speed of ethanol, n-heptane, iso-octane air mixtures. JSAE paper, 20068518.
[6] Liao, S. Y., Jiang, D. M., & Cheng, Q. (2004). Determination of laminar burning velocities for natural gas. Fuel, 83(9), 1247-1250.
[7] Bougrine, S., Richard, S., Nicolle, A., & Veynante, D. (2011). Numerical study of laminar flame properties of diluted methane-hydrogen-air flames at high pressure and temperature using detailed chemistry. international journal of hydrogen energy, 36(18), 12035-12047.
[8] Gülder, Ö. L. (1984). *Correlations of laminar combustion data for alternative SI engine fuels* (No. 841000). SAE Technical Paper.
[9] Hann, S., Grill, M., & Bargende, M. (2018). Reaction Kinetics Calculations and Modeling of the Laminar Flame Speeds of Gasoline Fuels. SAE Technical Paper, 2018-01-0857.
[10] Amirante, R., Distaso, E., Tamburrano, P., & Reitz, R. D. (2017). Laminar flame speed correlations for methane, ethane, propane and their mixtures, and natural gas and gasoline for spark-ignition engine simulations. International Journal of Engine Research, 18(9), 951-970.
[11] De Bellis, V., Bozza, F., & Tufano, D. (2017). A Comparison Between Two Phenomenological Combustion Models Applied to Different SI Engines (No. 2017-01-2184). SAE Technical Paper.
[12] Teodosio, L., Pirrello, D., Berni, F., De Bellis, V., Lanzafame, R., & D'Adamo, A. (2018). Impact of intake valve strategies on fuel consumption and knock tendency of a spark ignition engine. Applied Energy, 216, 91-104.
[13] Bozza, F, Teodosio, L, De Bellis, V, Fontanesi, S, & Iorio, A. (2018). Refinement of a 0D Turbulence Model to Predict Tumble and Turbulent Intensity in SI Engines. Part II: Model Concept, Validation and Discussion (No. 2018-01-0856). SAE Technical Paper.
[14] Bozza, F., De Bellis, V., Giannattasio, P., Teodosio, L., & Marchitto, L. (2017). Extension and Validation of a 1D Model Applied to the Analysis of a Water Injected Turbocharged Spark Ignited Engine at High Loads and over a WLTP Driving Cycle. *SAE International Journal of Engines*, *10*(2017-24-0014), 2141-2153.
[15] Liu, Y. D., Jia, M., Xie, M. Z., & Pang, B. (2013). Development of a new skeletal chemical kinetic model of toluene reference fuel with application to gasoline surrogate fuels for computational fluid dynamics engine simulation. Energy & Fuels, 27(8), 4899-4909.